Supporting Information

Compact Si/C Anodes Fabricated by Simultaneously Regulating the Size and Oxidation Degree of Si for Li-Ion Batteries

Liang Zhao [a, b], Yan-Bing He [a,*], Chengfei Li [a], Kelin Jiang [a], Peng Wang [a], Jiabin Ma [a, b], Heyi Xia [a, b], Fangyuan Chen [a], Yuanbiao He [a], Zhen Chen [a], Conghui You [a], and Feiyu Kang [a, b,*]

[a]Shenzhen Geim Graphene Center, Tsinghua Shenzhen International Graduate School, Tsinghua University, Shenzhen 518055, PR China.

[b]Laboratory of Advanced Materials, Department of Materials Science and Engineering, Tsinghua University, Beijing 100084, PR China.

* Corresponding author. E-mail address: he.yanbing@sz.tsinghua.edu.cn (Y.-B. He)

fykang@mail.tsinghua.edu.cn（F. Y. Kang）

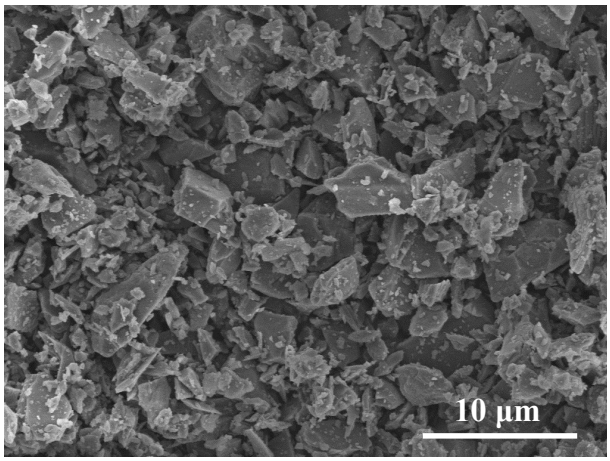

Fig. S1 SEM image of the micro-Si particles.

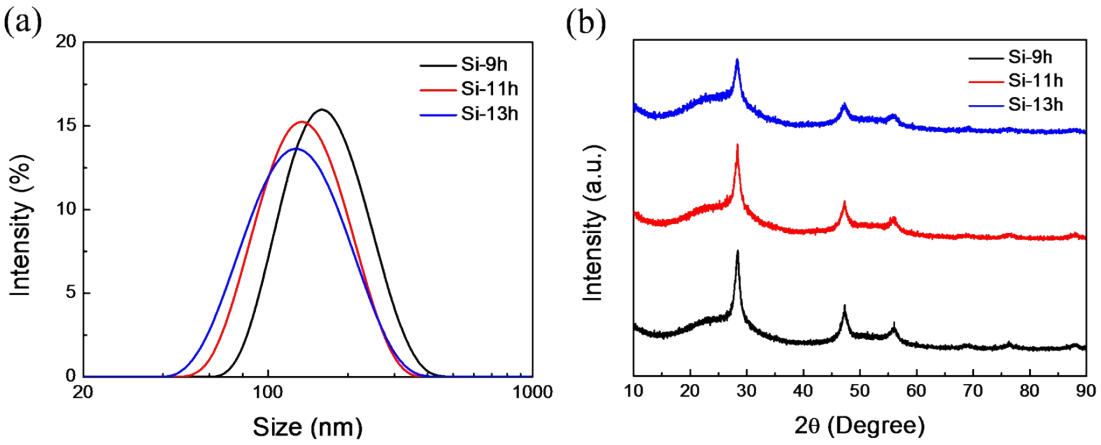

Fig. S2 (a) The PSD curves and (b) XRD patterns of Si-9h, Si-11h, and Si-13h.

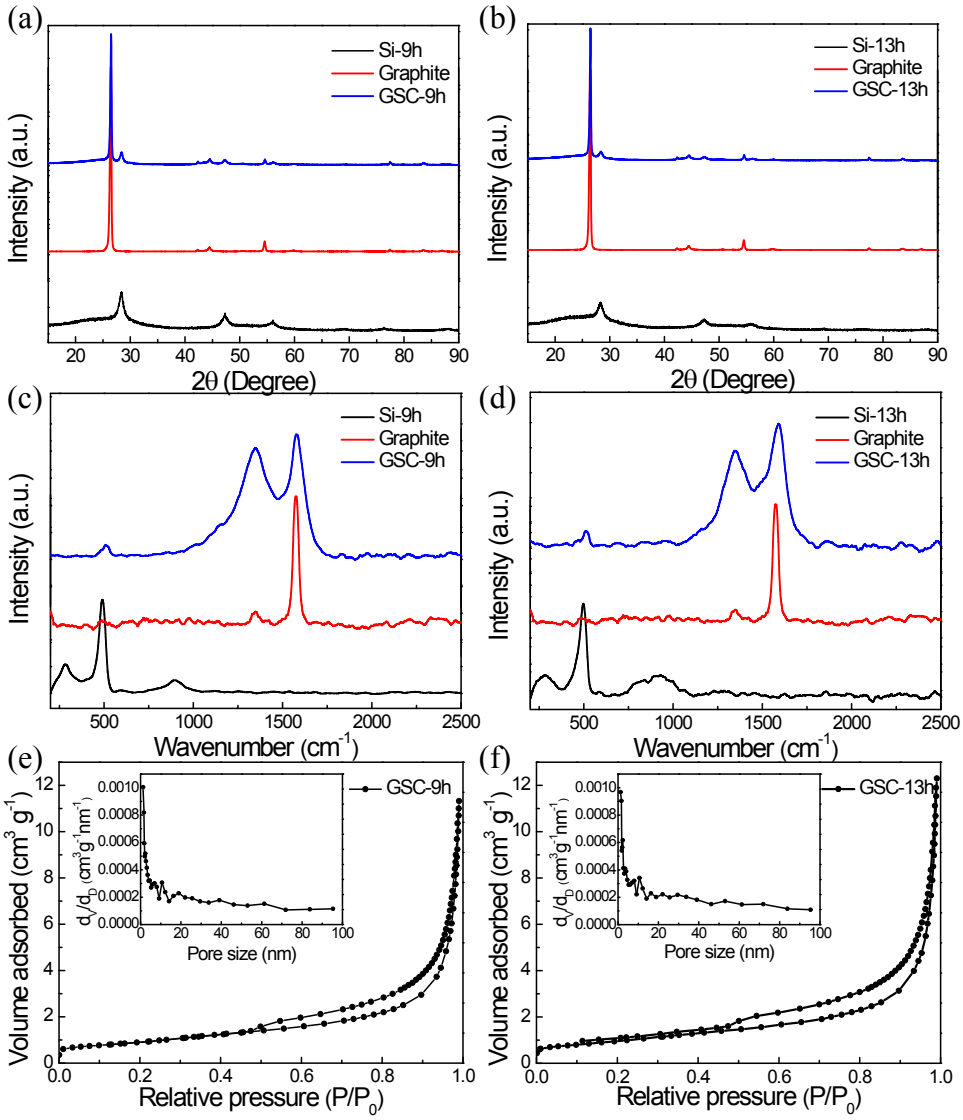

Fig. S3 (a, b) XRD patterns, (c, d) Raman spectra, and (e, f) BET plots of GSC-9h (a, c, e) and GSC-13h (b, d, f).

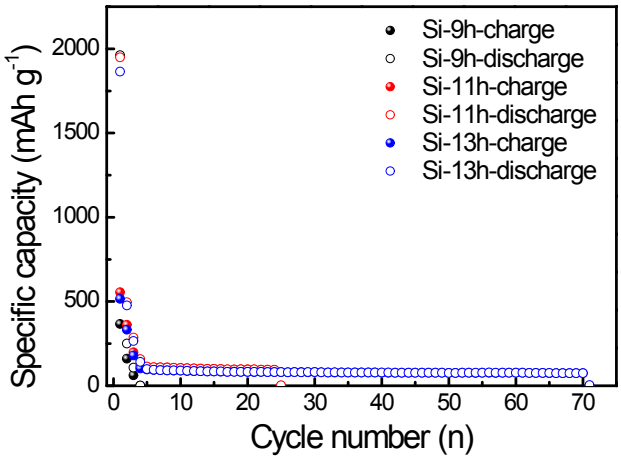

Fig. S4 Cycling performance of Si-9h, Si-11h, and Si-13h.

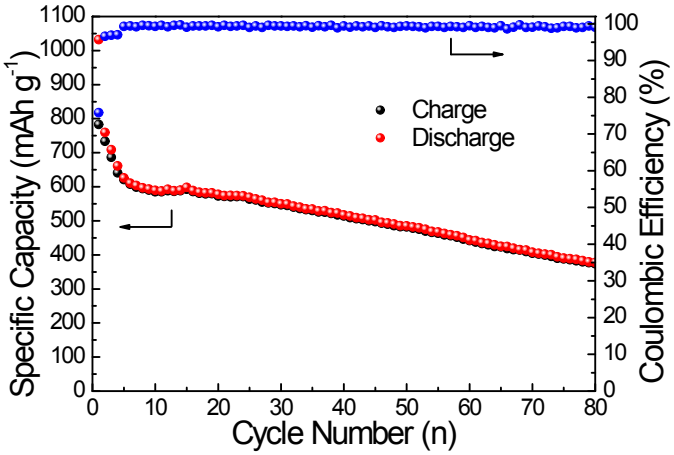

Fig. S5 Cycling performance of SC-11h.

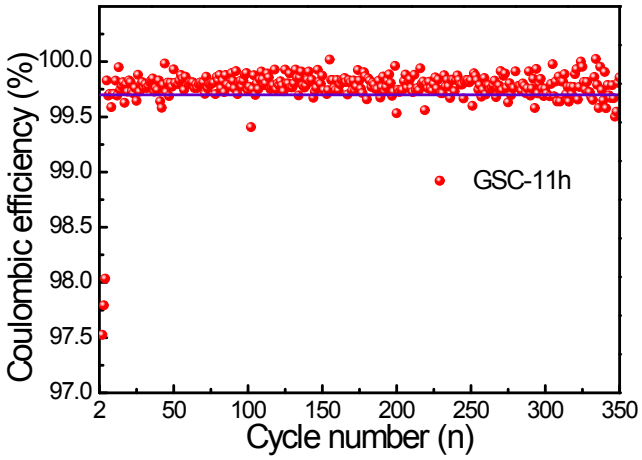

Fig. S6 Coulombic efficiency of GSC-11h from 2nd to 350th cycle.

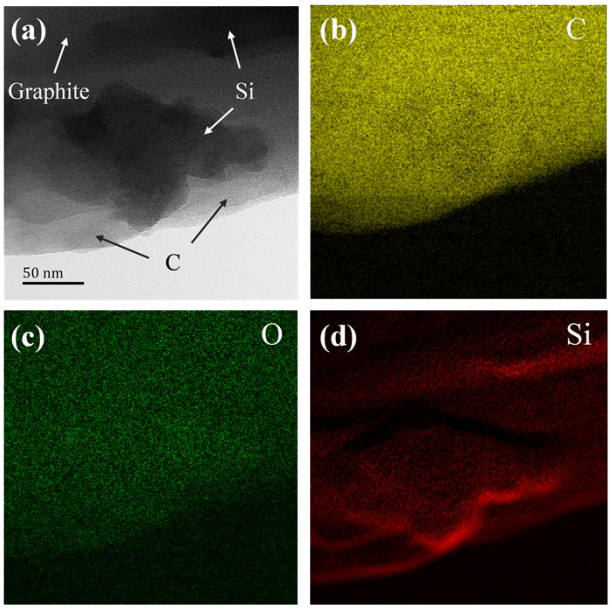

Fig. S7 (a) TEM and (c-d) EF-TEM images of the GSC-11h after 200 cycles.

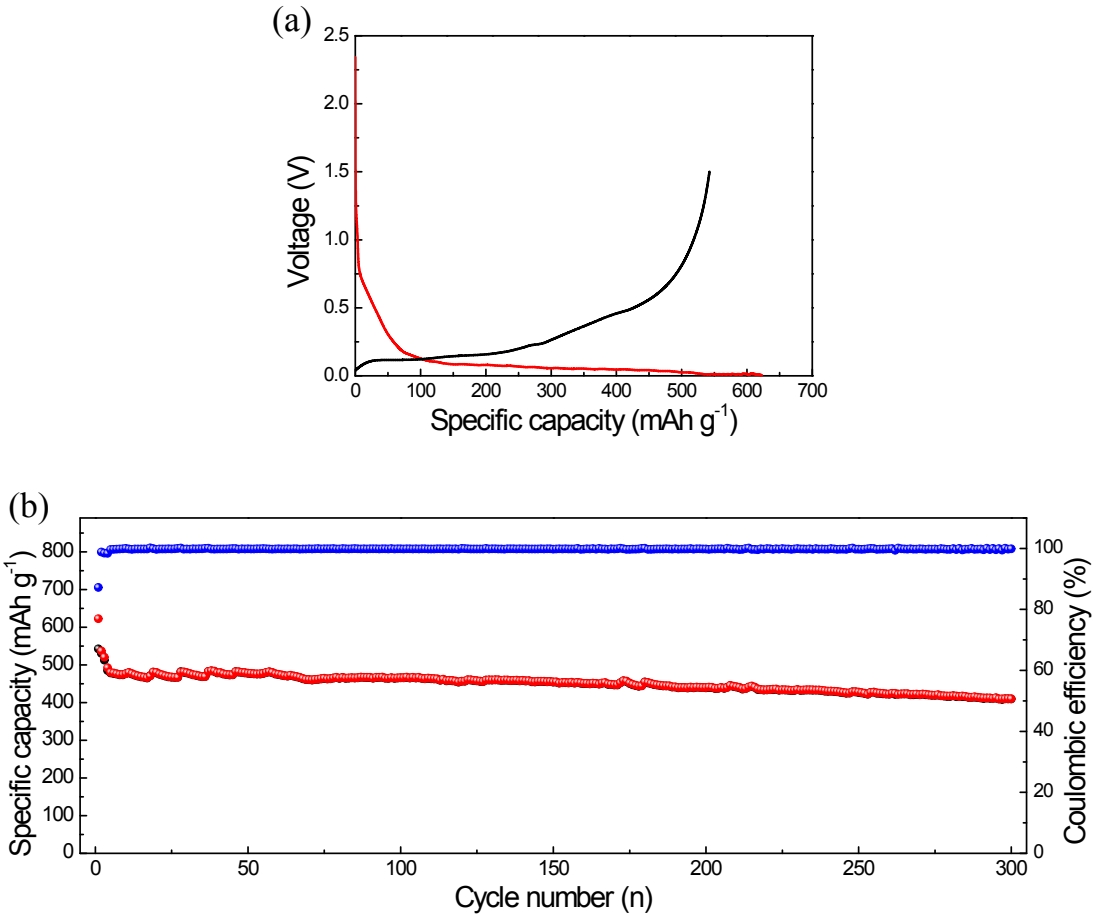

Fig. S8 (a) The initial charge and discharge curves and (b) cycling performance of the GSC-graphite anode.

Fig. S9 The optical photograph of $LiNi_{0.5}Co_{0.2}Mn_{0.3}O_2$/GSC-graphite full batteries.

Table S1 The proportion of different valence states of Si in GSC-9h, GSC-11h, and GSC-13h according to the XPS results in Figure 3e.

	Si^0	Si^{1+}	Si^{2+}	Si^{3+}	Si^{4+}
GSC-9h	17.6%	4.64%	31.03%	25.28%	21.45%
GSC-11h	14.46%	5.37%	29.02%	31.34%	19.82%
GSC-13h	11.99%	8.44%	29.12%	36.23%	14.23%

Table S2 The EIS simulation results of Figure 4d.

	R_b [Ω]	R_{SEI} [Ω]	R_{ct} [Ω]	R_t [Ω]
GSC-9h	2.92	4.05	10.71	17.68
GSC-11h	4.11	3.75	8.08	15.94
GSC-13h	4.38	2.48	15.37	22.23

Table S3 The EIS simulation results of Figure 6d.

	R_b [mΩ]	R_{SEI} [mΩ]	R_{ct} [mΩ]	R_t [mΩ]
1st	43.76	3.53	58.00	105.29
50th	46.20	12.01	10.83	69.04